



Please cite the Published Version

Bradburn, Steven, Murgatroyd, Christopher  and Ray, Nicola  (2019) Neuroinflammation in mild cognitive impairment and Alzheimer's disease: a meta-analysis. *Ageing Research Reviews*, 50. pp. 1-8. ISSN 1568-1637

DOI: <https://doi.org/10.1016/j.arr.2019.01.002>

Publisher: Elsevier

Version: Accepted Version

Downloaded from: <https://e-space.mmu.ac.uk/622107/>

Usage rights:  [Creative Commons: Attribution-Noncommercial-No Derivative Works 4.0](https://creativecommons.org/licenses/by-nc-nd/4.0/)

Additional Information: This is an Author Accepted Manuscript of a paper accepted for publication in *Ageing Research Reviews*, published by and copyright Elsevier.

Enquiries:

If you have questions about this document, contact openresearch@mmu.ac.uk. Please include the URL of the record in e-space. If you believe that your, or a third party's rights have been compromised through this document please see our Take Down policy (available from <https://www.mmu.ac.uk/library/using-the-library/policies-and-guidelines>)

Title: Meta-analysis of neuroinflammation in mild cognitive impairment and Alzheimer's disease

Authors:

Steven Bradburn^{a*}, Nicola Ray^b, Christopher Murgatroyd^a

^a Bioscience Research Centre, Manchester Metropolitan University, Manchester, United Kingdom.

^b Department of psychology, Manchester Metropolitan University, Manchester, United Kingdom.

***Corresponding author:** Dr Steven Bradburn, Bioscience Research Centre, Manchester Metropolitan University, Manchester, United Kingdom. Steven.bradburn@mmu.ac.uk.

Abstract (150 words)

Introduction

Increasing imaging evidence supports the role of neuroinflammation in dementia pathogenesis.

Despite this, the spatial association within the brain has not been comprehensively meta-analysed.

Methods

We searched literature databases for case-control studies examining the levels of translocator protein (TSPO) levels, representing neuroinflammation, in region of interest analyses between healthy controls and mild cognitive impairment (MCI) or Alzheimer's disease (AD) subjects.

Standardised mean difference effect sizes were calculated and results meta-analysed using random-effects models.

Results

The literature search identified 28 studies for inclusion, covering 37 different brain regions of interest. Compared to healthy controls, AD subjects had widespread increased TSPO levels throughout the brain, with the largest effects seen in fronto-temporo-parieto-occipital regions. MCI subjects also had increased TSPO levels, mainly within the neocortex, however, the effects were more modest.

Discussion

Neuroinflammation effect sizes increases and disperses from MCI to AD, relative to healthy controls.

Keywords (5 - 15)

Mild cognitive impairment, Alzheimer's disease, neuroinflammation, meta-analysis, translocator protein, positron emission tomography, neuroimaging

1. Introduction

Alongside the classical pathological hallmarks of Alzheimer's disease (AD), such as misfolded and aggregated proteins, neuroinflammation is appreciated as a major driver in disease pathogenesis and progression [1,2]. Genetic variants in inflammatory-related genes, such as those central to microglial function, have been implicated in AD [3]. Further, there is a reduced risk of AD in those taking non-steroidal anti-inflammatory drugs (NSAIDs) long-term, albeit at the epidemiological level [4]. Therefore, understanding the neuroinflammatory involvement during dementia is of high interest for both disease monitoring and therapeutic interventions.

Microglia and astrocytes are the predominant mediators of inflammation within the central nervous system, applicable to their ability to respond to neuropathologies [5,6], and have been prime candidates to investigate the neuroinflammatory process during disease pathogenesis. Over recent years, a great deal of attention has shifted to neuroimaging approaches which, unlike histological analyses, can elaborate on the morphological effects in living patients [7]. Specifically, positron emission tomography (PET) advances have been integral in quantifying levels of inflammation throughout the brain during dementia and have revealed neuroinflammation as one of the earliest detectable biomarkers in the disease [2,8].

The translocator protein-18 kDa (TSPO) is a transmembrane domain protein found on the outer mitochondrial membrane. It is widely distributed in various tissues, with minimal expression within the brain at physiological levels [9]. Upon microglial and astrocyte activation TSPO levels are significantly increased [10,11], supporting TSPO detection as an *in vivo* marker of neuroinflammation. Since the first use of TSPO ligands in PET on AD subjects by Groom and colleagues at the turn of the 21st century [12], numerous groups have added further reports through the use of various TSPO ligands (as reviewed in [7]). However, reports so far concern analyses on study-specific regions of interest, restricting the interpretation of morphological differences in

neuroinflammation during MCI and AD. Further, due to the demanding nature of PET protocols, studies often contain relatively few ($n < 10$) subjects [12–17], thus limiting the power of analyses.

In this regard, we performed the first meta-analyses concerning all brain regions reported in studies investigating TSPO levels in MCI and AD to provide a comprehensive analysis with increased statistical power.

2. Methods

2.1. Search strategy

All meta-analyses were performed according to the Preferred Reporting Items for Systematic Reviews and Meta-analyses (PRISMA) guidelines [18]. PubMed and Scopus literature databases were searched, up to 31st July 2018, and were restricted to journal articles written in English.

Search terms used to find potential articles were as follows: (“Positron-emission tomography” OR “PET”) AND (“TSPO” OR “Translocator Protein” OR “18 kDa” OR “Neuroinflammation” OR “PK11195” OR “microglia” OR “benzodiazepine”) AND (“Alzheimer’s disease” OR “dementia” OR “cognitive impairment” OR “MCI” OR “Prodromal”). We also manually searched any included articles for additional relevant references. A standardised review protocol has not been published.

2.2. Eligibility criteria

Studies were included in the meta-analysis based on the following criteria: (1) written in English, (2) measured TSPO binding using PET; (3) participants were stratified into healthy control (HC) and MCI and/or AD groups; (4) performed a region of interest analysis; (5) TSPO levels were reported.

We excluded studies if they: (1) were of an interventional study design; (2) contained a duplicate study population; (3) did not perform a region of interest analysis.

2.3. Data extraction

The following data was extracted from each included study: (1) the TSPO ligand used; (2) the outcome used to measure TSPO levels; (3) the number of subjects in each group; (4) the average age of subjects in each group; (5) the proportion of female subjects in each group; (6) the average MMSE scores of subjects in each group; (7) the average value and standard deviation (SD) for the outcome of TSPO activation in each group.

Where studies reported separate results for both hemispheres [19,20], results were averaged across hemispheres. When studies reported results in graphical format [13,14,21,22], mean and SD values were estimated by using the measurement tool in Adobe Reader (v.2018.011.20058). One study [20] presented their data as mean with 95% CI in a graphical format, therefore the corresponding author was contacted to request the raw tabulated data, which they kindly provided. One study reported standard error (SE) [23], as opposed to SD, therefore values were converted to SD using the following formula: $SD = SE \times \sqrt{N}$. Where multiple studies utilised the same study population, we selected the study containing the larger study population for inclusion and excluded the duplicate population. One study [24] reported combined results for the MCI and AD groups in a graphical format, therefore the corresponding author was contacted for separate results in mean and SD tabulated format, which they kindly provided.

2.4. Quality assessment

The quality of included studies was assessed using the Newcastle-Ottawa quality assessment scale for case-control studies [25]. A maximum score of 9 can be awarded, whereby studies with ≥ 7 points are generally considered to be of high quality. The criteria for the assessment scale can be found in the supplementary material.

2.5. Statistical analysis

Meta-analysis was performed using the *metafor* package in R [26], when there were ≥ 2 studies for the same region of interest. Since TSPO levels were determined using different PET ligands and

analytical methods, results were converted to standardised mean differences (SMD) between controls and MCI or AD groups. A positive result indicates higher TSPO levels in the cases (AD or MCI), compared to the healthy controls (HC). Results were meta-analysed using a random-effects model and are reported as SMD and 95% confidence intervals (CI).

Statistical heterogeneity across studies was assessed using the I^2 statistic. Subgroup analysis was performed to investigate the potential source of heterogeneity. Specifically, we anticipated the majority of variation to be explained by the type of TSPO ligand used, since second generation TSPO ligands offer superior neuroimaging characteristics, such as increased sensitivity and signal to noise ratios, compared to the initial generation [27]. We therefore stratified studies in two: 1st generation ([¹¹C]PK11195 or [¹¹C](R)-PK11195) or 2nd generation ([¹¹C]DAA1106, [¹¹C]Vinpocetine, [¹¹C]PBR28, [¹⁸F]FEDAA1106, [¹⁸F]DPA-714, [¹⁸F]FEPPA, [¹⁸F]FEMPA, [¹¹C]DPA713) TSPO ligands. We also performed subgroup analysis based on study quality scores (<7 points / ≥ 7 points).

Sensitivity analysis was conducted on those regions which reached statistical significance to assess the robustness of the result. Specifically, the leave-1-out method was applied which repeated the random effects model by leaving out one study at a time. The results of this analysis are reported as the number of studies which can be removed without affected the significance of the model.

Mixed-effects meta-regressions were performed, through the *rma* function, when the number of studies permitted (≥ 10 studies) to determine the relationship between SMD and patient MMSE scores, a proxy of disease severity.

Publication bias was tested when the number of studies permitted (> 2 studies), through the Egger regression test. Models which were significant after publication bias testing were further entered into trim-and-fill analysis. This method aims to identify and correct for funnel plot asymmetry by imputing possible missing studies.

3. Results

3.1. Study selection

Following the literature searches, 528 articles were returned, of which 455 were excluded based on title and abstract suitability (Figure 1). After removal of duplicate results, the full text of 40 articles was examined. Following this, 13 articles were excluded because they did not meet our inclusion criteria, and 27 articles were eligible for inclusion in the meta-analyses.

One article [28] reported results from two independent studies using different TSPO ligands, therefore these were treated as two separate studies. Overall, 28 studies were meta-analysed, of which 13 and 23 studies contained MCI and AD groups, respectively.

3.2. Study characteristics

The overall study characteristics of interest, including the type of PET ligand used, outcome, number of subjects, age of subjects, proportion of female subjects and subject MMSE scores for each included study is presented in Table 1. Quality scores of the included studies ranged between 4 - 9 points (Supplementary Table 1), with the majority being of high quality ≥ 7 points.

In total there were 37 regions of interest which were eligible for meta-analysis. These regions are defined as: amygdala, anterior cingulate (including: cortex and gyrus), caudate, cerebellum, cortex (including: averaged cerebral cortex, cortical and whole cortex), entorhinal, frontal (including: cortex and lobe), gray matter, hippocampus, inferior and middle temporal (including: gyri and cortex), insula, lateral temporal, lingual gyrus, medial temporal (including: region, cortex, lobe, pole), midbrain, middle frontal (including: cortex and gyrus), occipital (including: cortex, lobe and lateral region), orbitofrontal, pallidum, parahippocampal (including: cortex and gyrus), parietal (including: lobe, cortex, and lateral), inferior parietal (including: lobule and cortex), superior parietal (including: cortex and gyrus), posterior cingulate (including: gyrus and cortex), posterior temporal (including: lobe and cortex), precuneus, prefrontal cortex (including: dorsolateral and lateral), pons, putamen, sensorimotor cortex, striatum, superior frontal (including cortex and gyrus), superior temporal

(including cortex and gyrus), temporal (including: cortex and lobe), thalamus, white matter (including: averaged cerebral white matter), whole brain.

3.3. Meta-analysis between HC and AD subjects

For the comparison between the HC and AD groups, 36 regions of interest were eligible for meta-analysis, of which 27 regions had significantly higher TSPO levels in the AD subjects compared to the HC subjects (Figure 2, Table 2). The largest effects were seen in frontal, temporal, parietal and occipital regions, whilst the smallest effects were found in the thalamus, cerebellum and pons (Figure 2, Table 2). There were no differences in the putamen, cortex, lingual gyrus, caudate, insula, midbrain, sensorimotor cortex, white matter or gray matter.

Sensitivity analysis through leave-1-out found the cerebellum, orbitofrontal cortex, pallidum, pons, striatum, entorhinal and lateral temporal region model effects were affected by one or more study exclusions (Supplementary Table 2).

Publication bias was evident in the amygdala, anterior cingulate, posterior cingulate, middle frontal, prefrontal cortex, superior frontal, superior parietal, precuneus, entorhinal, inferior and middle temporal and parahippocampal regions (Supplementary Table 2). Apart from the amygdala model, imputing potential missing studies through trim-and-fill analysis failed to change these overall model effects (Supplementary Table 2).

Significant study heterogeneity was detected in the majority of models (Table 2). To investigate potential sources of heterogeneity, subgrouping was performed for study quality (<7 / ≥ 7 quality score) and the type of TSPO ligand used (1st generation / 2nd generation). Heterogeneity in the anterior cingulate, caudate, superior frontal, parietal, putamen, hippocampus, inferior and middle temporal, lateral temporal and thalamus models were reduced when stratified by TSPO ligand type (Supplementary table 3). Further, when stratified by study quality, heterogeneity within the anterior cingulate, posterior cingulate, cerebellum, cortex, occipital, parietal, precuneus, putamen,

hippocampus, inferior and middle temporal, parahippocampal and thalamus region models were reduced (Supplementary table 4).

Meta-regression analysis was performed in models with ≥ 10 included studies to determine the association of AD subject MMSE scores with SMD effect sizes. There was no significant association in the anterior cingulate (estimate: -0.03; 95% CI: -0.19 - 0.13; $P = 0.678$), posterior cingulate (estimate: -0.10; 95% CI: -0.22 - 0.01; $P = 0.086$), cerebellum (estimate: -0.09; 95% CI: -0.21 - 0.04; $P = 0.189$), occipital (estimate: -0.11; 95% CI: -0.23 - 0.01; $P = 0.082$), thalamus (estimate: -0.03; 95% CI: -0.15 - 0.09; $P = 0.558$) or hippocampus (estimate: -0.02; 95% CI: -0.18 - 0.13; $P = 0.769$) region models. However, there was a negative association between MMSE scores and SMD effect sizes in the parietal region model (estimate: -0.11, 95% CI: -0.21 - -0.02; $P = 0.024$, Figure 3).

3.4. Meta-analysis between HC and MCI subjects

There were 22 regions of interest meta-analysed for the comparisons between MCI and HC subjects (Figure 2, Table 3). From these, the MCI subjects had significantly more TSPO levels within the anterior cingulate, posterior cingulate, frontal, occipital, inferior parietal, precuneus, temporal, hippocampus, lateral temporal, medial temporal, thalamus and whole brain regions compared to HC subjects (Figure 2, Table 3). There were no differences in the amygdala, cerebellum, prefrontal cortex, superior parietal, sensorimotor cortex, striatum, entorhinal, inferior and middle temporal, parahippocampal and superior temporal regions between the groups (Figure 2, Table 3).

Leave-1-out analysis was performed on the significant models and found that the anterior cingulate, lateral temporal and whole brain models were dependent on one or more studies included in the model (Supplementary Table 5). The posterior cingulate, frontal, occipital, parietal, precuneus, temporal, hippocampus, medial temporal and thalamus regions were unaffected by single study exclusions.

Publication bias was only evident in the amygdala and striatum models (Supplementary Table 5).

Despite this, trim-and-fill analysis failed to impute any missing studies (Supplementary Table 5).

Significant study heterogeneity was only evident in the amygdala model (Table 3). However, this heterogeneity was not explained by the type of TSPO ligand used (Supplementary Table 6) or the quality of the included studies (Supplementary Table 7).

Meta-regression was only performed on the posterior cingulate, which failed to report an association between patient MMSE scores and SMD values (estimate: -0.06; 95% CI: -0.26 - 0.14; P = 0.536).

4. Discussion

The present meta-analysis contained 28 studies covering 37 different brain regions of interest for levels of neuroinflammation in AD and MCI, relative to controls. Levels of neuroinflammation were higher and more disperse in AD, whereas only modest levels were detected in MCI, primarily within the neocortex. Further, in studies concerning AD subjects, effect sizes were associated with disease severity (MMSE scores) in the parietal region. Collectively, these results are in agreement with recent reports of an increase in neuroinflammation with disease pathogenesis [2,29].

The latest hypothesis suggests levels of neuroinflammation peaks early on, possibly reflecting an initial anti-inflammatory response, following by a second peak during AD progression, which may indicate a pro-inflammatory shift [2,29,30]. This complex relationship may be due to the microglial reaction to the deposition and propagation of amyloid and hyperphosphorylated tau pathologies. Both amyloid and tau can be internalised by and activate microglia [5,6]. But, evidence suggests the spatio-temporal severity of each may decide upon the inflammatory state produced. For example, PET studies utilising TSPO and amyloid or tau ligands have shown strong inter-relationships of neuroinflammation with amyloid levels in early MCI [20,29–32], with little [32] or no correlations [31] with tau levels. This inflammatory peak during the prodromal phase may reflect the anti-

inflammatory response of microglia to amyloid. Amyloid deposition is initially seen throughout the neocortex, before expanding ventrally into the allocortex, midbrain, brainstem and eventually into cerebellar areas [33]. This pattern is in agreement with our results in the MCI subjects, where increased neuroinflammation was seen predominantly within regions associated with early amyloid deposition (e.g. frontal, occipital, parietal, temporal), whereas regions generally associated with later stages were less affected (e.g. striatum and cerebellum). On the other hand, neuroinflammation and tau associations are much more closely aligned in AD, than they are in MCI [32]. Histological analyses also support this linear association of microgliosis with tau tangle burden during disease severity [34]. Again, our results corroborate the spatial propagation of tau during AD with all of the temporal regions affected by high effects of neuroinflammation, a region dominated with exacerbated tau aggregation during the disease course [35]. Collectively therefore, the spatial pattern of neuroinflammation during AD may be a reaction to initial amyloid deposition in the earlier phases, with a second hit during later tau spreading.

A conceivable weakness of current PET studies targeting TSPO is that the ligands used can only indicate the activation level of those regions of interest, rather they are unable to differentiate between pro- and anti-inflammatory states of microglia and astrocytes. Future developments of ligands that can discriminate these inflammatory states, such as the promising recent insights into P2Y₁₂R and P2X₇R receptor targeting [36], will be vital in elucidating these associations with disease pathogenesis and further aid with potential therapy monitoring [37].

Another noteworthy finding from our analyses is the cerebellum as a region with significantly increased TSPO binding in the AD subjects. The cerebellum is often selected as a reference region during TSPO PET image analysis [12,21,30,38,39], mainly due to the belief that this region is relatively spared from AD pathology. Based on our findings, we would not recommend this structure as an appropriate reference region. For an alternative reference during image analysis, our results suggest the caudate (6 studies) or white matter (5 studies) may be a better alternative to the

cerebellum. The lack of TSPO signal differences in the caudate, for example, is also corroborated in an early report describing no difference in the number of microglia between control and AD caudate brain tissue [40].

Despite the strengths of the current investigation, it is important to address some important limitations. One challenge is that some of the regions of interest contained relatively few studies, especially involving MCI subjects, which can restrict the power of these analyses and limit publication bias analyses. Clearly, additional studies, particularly involving MCI subjects covering more regions of interest are warranted. Additionally, the included studies measured TSPO levels through a variety of analytical methods and different ligands. We did, however, anticipate such heterogeneity by applying random-effect models throughout and performing *post-hoc* subgroup analyses.

Collectively, our findings are in agreement with the recent dual inflammatory hit hypothesis during AD progression. Further work concerning longitudinal PET analysis and additional ligand development is needed in the prodromal AD phases to fully understand the spatio-temporal sequence of neuroinflammatory events.

Acknowledgements

We would like to thank Dr's Parbo and Passamonti for kindly agreeing to and providing the requested data to enable their study inclusion within the analysis.

Funding

This research did not receive any specific grant from funding agencies in the public, commercial, or not-for-profit sectors.

Research in context (150 words)

- 1. Systematic review:** Using PubMed and Scopus databases, we reviewed the literature regarding levels of neuroinflammation, as measured by translocator protein binding during

positron emission tomography, in mild cognitive impairment and Alzheimer's disease.

Despite recent systematic reviews on the topic, no meta-analysis has been performed.

- 2. Interpretation:** From an analysis involving 28 studies spanning a total of 37 brain regions of interest, we discovered increased and widespread neuroinflammation in Alzheimer's disease, with less effects in those with mild cognitive impairment, when compared to healthy controls.
- 3. Future directions:** Future studies are needed for certain regions of interest containing low numbers of studies, especially involving mild cognitive impairment cases. Further, the development of inflammatory state specific ligands are warranted. Doing so will increase the statistical power of future meta-analyses and aid in identifying more regions impacted with neuroinflammation early in disease pathogenesis.

References [50 max.]

- [1] Heneka MT, Carson MJ, El Khoury J, Landreth GE, Brosseron F, Feinstein DL, et al. Neuroinflammation in Alzheimer's disease. *Lancet Neurol* 2015;14:388–405. doi:10.1016/S1474-4422(15)70016-5.
- [2] Calsolaro V, Edison P. Neuroinflammation in Alzheimer's disease: Current evidence and future directions. *Alzheimer's & Dementia* 2016;12:719–32. doi:10.1016/j.jalz.2016.02.010.
- [3] Villegas-Llerena C, Phillips A, Garcia-Reitboeck P, Hardy J, Pocock JM. Microglial genes regulating neuroinflammation in the progression of Alzheimer's disease. *Current Opinion in Neurobiology* 2016;36:74–81. doi:10.1016/j.conb.2015.10.004.
- [4] Zhang C, Wang Y, Wang D, Zhang J, Zhang F. NSAID Exposure and Risk of Alzheimer's Disease: An Updated Meta-Analysis From Cohort Studies. *Front Aging Neurosci* 2018;10. doi:10.3389/fnagi.2018.00083.

- [5] Morales I, Jiménez JM, Mancilla M, Maccioni RB. Tau oligomers and fibrils induce activation of microglial cells. *J Alzheimers Dis* 2013;37:849–56. doi:10.3233/JAD-131843.
- [6] Meda L, Cassatella MA, Szendrei GI, Jr LO, Baron P, Villalba M, et al. Activation of microglial cells by β -amyloid protein and interferon- γ . *Nature* 1995;374:647–50. doi:10.1038/374647a0.
- [7] Lagarde J, Sarazin M, Bottlaender M. In vivo PET imaging of neuroinflammation in Alzheimer's disease. *J Neural Transm* 2018;125:847–67. doi:10.1007/s00702-017-1731-x.
- [8] Okello A, Edison P, Archer HA, Turkheimer FE, Kennedy J, Bullock R, et al. Microglial activation and amyloid deposition in mild cognitive impairment: a PET study. *Neurology* 2009;72:56–62. doi:10.1212/01.wnl.0000338622.27876.0d.
- [9] Banati RB. Visualising microglial activation in vivo. *Glia* 2002;40:206–17. doi:10.1002/glia.10144.
- [10] Lavisse S, Guillermier M, Hérard A-S, Petit F, Delahaye M, Van Camp N, et al. Reactive astrocytes overexpress TSPO and are detected by TSPO positron emission tomography imaging. *J Neurosci* 2012;32:10809–18. doi:10.1523/JNEUROSCI.1487-12.2012.
- [11] Wilms H, Claasen J, Röhl C, Sievers J, Deuschl G, Lucius R. Involvement of benzodiazepine receptors in neuroinflammatory and neurodegenerative diseases: evidence from activated microglial cells in vitro. *Neurobiol Dis* 2003;14:417–24.
- [12] Groom GN, Junck L, Foster NL, Frey KA, Kuhl DE. PET of peripheral benzodiazepine binding sites in the microgliosis of Alzheimer's disease. *J Nucl Med* 1995;36:2207–10.
- [13] Gulyás B, Vas A, Tóth M, Takano A, Varrone A, Cselényi Z, et al. Age and disease related changes in the translocator protein (TSPO) system in the human brain: positron emission tomography measurements with [^{11}C]vinpocetine. *Neuroimage* 2011;56:1111–21. doi:10.1016/j.neuroimage.2011.02.020.
- [14] Wiley CA, Lopresti BJ, Veneti S, Price J, Klunk WE, DeKosky ST, et al. Carbon 11-labeled Pittsburgh Compound B and carbon 11-labeled (R)-PK11195 positron emission tomographic imaging in Alzheimer disease. *Arch Neurol* 2009;66:60–7. doi:10.1001/archneurol.2008.511.

- [15] Varrone A, Mattsson P, Forsberg A, Takano A, Nag S, Gulyás B, et al. In vivo imaging of the 18-kDa translocator protein (TSPO) with [18F]FEDAA1106 and PET does not show increased binding in Alzheimer's disease patients. *Eur J Nucl Med Mol Imaging* 2013;40:921–31. doi:10.1007/s00259-013-2359-1.
- [16] Golla SSV, Boellaard R, Oikonen V, Hoffmann A, van Berckel BNM, Windhorst AD, et al. Quantification of [18F]DPA-714 binding in the human brain: initial studies in healthy controls and Alzheimer's disease patients. *J Cereb Blood Flow Metab* 2015;35:766–72. doi:10.1038/jcbfm.2014.261.
- [17] Femminella GD, Ninan S, Atkinson R, Fan Z, Brooks DJ, Edison P. Does Microglial Activation Influence Hippocampal Volume and Neuronal Function in Alzheimer's Disease and Parkinson's Disease Dementia? *J Alzheimers Dis* 2016;51:1275–89. doi:10.3233/JAD-150827.
- [18] Liberati A, Altman DG, Tetzlaff J, Mulrow C, Gøtzsche PC, Ioannidis JPA, et al. The PRISMA statement for reporting systematic reviews and meta-analyses of studies that evaluate healthcare interventions: explanation and elaboration. *BMJ* 2009;339:b2700. doi:10.1136/bmj.b2700.
- [19] Cagnin A, Brooks DJ, Kennedy AM, Gunn RN, Myers R, Turkheimer FE, et al. In-vivo measurement of activated microglia in dementia. *Lancet* 2001;358:461–7. doi:10.1016/S0140-6736(01)05625-2.
- [20] Parbo P, Ismail R, Hansen KV, Amidi A, Mårup FH, Gottrup H, et al. Brain inflammation accompanies amyloid in the majority of mild cognitive impairment cases due to Alzheimer's disease. *Brain* 2017;140:2002–11. doi:10.1093/brain/awx120.
- [21] Kropholler MA, Boellaard R, van Berckel BNM, Schuitmaker A, Kloet RW, Lubberink MJ, et al. Evaluation of reference regions for (R)-[(11)C]PK11195 studies in Alzheimer's disease and mild cognitive impairment. *J Cereb Blood Flow Metab* 2007;27:1965–74. doi:10.1038/sj.jcbfm.9600488.

- [22] Tomasi G, Edison P, Bertoldo A, Roncaroli F, Singh P, Gerhard A, et al. Novel reference region model reveals increased microglial and reduced vascular binding of 11C-(R)-PK11195 in patients with Alzheimer's disease. *J Nucl Med* 2008;49:1249–56.
doi:10.2967/jnumed.108.050583.
- [23] Suridjan I, Pollock BG, Verhoeff NPLG, Voineskos AN, Chow T, Rusjan PM, et al. In-vivo imaging of grey and white matter neuroinflammation in Alzheimer's disease: a positron emission tomography study with a novel radioligand, [18F]-FEPPA. *Mol Psychiatry* 2015;20:1579–87.
doi:10.1038/mp.2015.1.
- [24] Passamonti L, Rodríguez PV, Hong YT, Allinson KSJ, Bevan-Jones WR, Williamson D, et al. [11C]PK11195 binding in Alzheimer disease and progressive supranuclear palsy. *Neurology* 2018;90:e1989–96. doi:10.1212/WNL.0000000000005610.
- [25] Wells G, Shea B, O'Connell D, Peterson J, Welch V, Losos M, et al. The Newcastle - Scale for assessing the quality of nonrandomised studies in meta-analyses.pdf 2000.
<http://www.medicine.mcgill.ca/rtamblyn/Readings/The%20Newcastle%20-%20Scale%20for%20assessing%20the%20quality%20of%20nonrandomised%20studies%20in%20meta-analyses.pdf> (accessed September 17, 2018).
- [26] Viechtbauer W. Conducting Meta-Analyses in R with the metafor Package. *Journal of Statistical Software* 2010;36. doi:10.18637/jss.v036.i03.
- [27] Alam MM, Lee J, Lee S-Y. Recent Progress in the Development of TSPO PET Ligands for Neuroinflammation Imaging in Neurological Diseases. *Nucl Med Mol Imaging* 2017;51:283–96.
doi:10.1007/s13139-017-0475-8.
- [28] Yokokura M, Terada T, Bunai T, Nakaizumi K, Takebayashi K, Iwata Y, et al. Depiction of microglial activation in aging and dementia: Positron emission tomography with [11C]DPA713 versus [11C](R)PK11195. *J Cereb Blood Flow Metab* 2017;37:877–89.
doi:10.1177/0271678X16646788.

- [29] Fan Z, Brooks DJ, Okello A, Edison P. An early and late peak in microglial activation in Alzheimer's disease trajectory. *Brain* 2017;140:792–803. doi:10.1093/brain/aww349.
- [30] Hamelin L, Lagarde J, Dorothée G, Leroy C, Labit M, Comley RA, et al. Early and protective microglial activation in Alzheimer's disease: a prospective study using 18F-DPA-714 PET imaging. *Brain* 2016;139:1252–64. doi:10.1093/brain/aww017.
- [31] Parbo P, Ismail R, Sommerauer M, Stokholm MG, Hansen AK, Hansen KV, et al. Does inflammation precede tau aggregation in early Alzheimer's disease? A PET study. *Neurobiol Dis* 2018;117:211–6. doi:10.1016/j.nbd.2018.06.004.
- [32] Dani M, Wood M, Mizoguchi R, Fan Z, Walker Z, Morgan R, et al. Microglial activation correlates in vivo with both tau and amyloid in Alzheimer's disease. *Brain* 2018. doi:10.1093/brain/awy188.
- [33] Thal DR, Rüb U, Orantes M, Braak H. Phases of A beta-deposition in the human brain and its relevance for the development of AD. *Neurology* 2002;58:1791–800.
- [34] Serrano-Pozo A, Mielke ML, Gómez-Isla T, Betensky RA, Growdon JH, Frosch MP, et al. Reactive glia not only associates with plaques but also parallels tangles in Alzheimer's disease. *Am J Pathol* 2011;179:1373–84. doi:10.1016/j.ajpath.2011.05.047.
- [35] Braak H, Alafuzoff I, Arzberger T, Kretschmar H, Del Tredici K. Staging of Alzheimer disease-associated neurofibrillary pathology using paraffin sections and immunocytochemistry. *Acta Neuropathol* 2006;112:389–404. doi:10.1007/s00401-006-0127-z.
- [36] Beaino W, Janssen B, Kooij G, van der Pol SMA, van Het Hof B, van Horsen J, et al. Purinergic receptors P2Y12R and P2X7R: potential targets for PET imaging of microglia phenotypes in multiple sclerosis. *J Neuroinflammation* 2017;14. doi:10.1186/s12974-017-1034-z.
- [37] Janssen B, Vugts D, Windhorst A, Mach R, Janssen B, Vugts DJ, et al. PET Imaging of Microglial Activation—Beyond Targeting TSPO. *Molecules* 2018;23:607. doi:10.3390/molecules23030607.
- [38] Lyoo CH, Ikawa M, Liow J-S, Zoghbi SS, Morse CL, Pike VW, et al. Cerebellum Can Serve As a Pseudo-Reference Region in Alzheimer Disease to Detect Neuroinflammation Measured with

PET Radioligand Binding to Translocator Protein. *J Nucl Med* 2015;56:701–6.

doi:10.2967/jnumed.114.146027.

- [39] Kreisl WC, Lyoo CH, Liow J-S, Snow J, Page E, Jenko KJ, et al. Distinct patterns of increased translocator protein in posterior cortical atrophy and amnesic Alzheimer's disease. *Neurobiol Aging* 2017;51:132–40. doi:10.1016/j.neurobiolaging.2016.12.006.
- [40] Falke E, Han L-Y, Arnold SE. Absence of neurodegeneration in the thalamus and caudate of elderly patients with schizophrenia. *Psychiatry Research* 2000;93:103–10. doi:10.1016/S0165-1781(00)00104-9.
- [41] Edison P, Archer HA, Gerhard A, Hinz R, Pavese N, Turkheimer FE, et al. Microglia, amyloid, and cognition in Alzheimer's disease: An [11C](R)PK11195-PET and [11C]PIB-PET study. *Neurobiol Dis* 2008;32:412–9. doi:10.1016/j.nbd.2008.08.001.
- [42] Yasuno F, Ota M, Kosaka J, Ito H, Higuchi M, Doronbekov TK, et al. Increased binding of peripheral benzodiazepine receptor in Alzheimer's disease measured by positron emission tomography with [11C]DAA1106. *Biol Psychiatry* 2008;64:835–41. doi:10.1016/j.biopsych.2008.04.021.
- [43] Yokokura M, Mori N, Yagi S, Yoshikawa E, Kikuchi M, Yoshihara Y, et al. In vivo changes in microglial activation and amyloid deposits in brain regions with hypometabolism in Alzheimer's disease. *Eur J Nucl Med Mol Imaging* 2011;38:343–51. doi:10.1007/s00259-010-1612-0.
- [44] Yasuno F, Kosaka J, Ota M, Higuchi M, Ito H, Fujimura Y, et al. Increased binding of peripheral benzodiazepine receptor in mild cognitive impairment-dementia converters measured by positron emission tomography with [¹¹C]DAA1106. *Psychiatry Res* 2012;203:67–74. doi:10.1016/j.psychresns.2011.08.013.
- [45] Kreisl WC, Lyoo CH, McGwier M, Snow J, Jenko KJ, Kimura N, et al. In vivo radioligand binding to translocator protein correlates with severity of Alzheimer's disease. *Brain* 2013;136:2228–38. doi:10.1093/brain/awt145.

- [46] Schuitemaker A, Kropholler MA, Boellaard R, van der Flier WM, Kloet RW, van der Doef TF, et al. Microglial activation in Alzheimer's disease: an (R)-[¹¹C]PK11195 positron emission tomography study. *Neurobiol Aging* 2013;34:128–36. doi:10.1016/j.neurobiolaging.2012.04.021.
- [47] Fan Z, Aman Y, Ahmed I, Chetelat G, Landeau B, Chaudhuri KR, et al. Influence of microglial activation on neuronal function in Alzheimer's and Parkinson's disease dementia. *Alzheimer's & Dementia: The Journal of the Alzheimer's Association* 2015;11:608-621.e7. doi:10.1016/j.jalz.2014.06.016.
- [48] Varrone A, Oikonen V, Forsberg A, Joutsa J, Takano A, Solin O, et al. Positron emission tomography imaging of the 18-kDa translocator protein (TSPO) with [18F]FEMPA in Alzheimer's disease patients and control subjects. *Eur J Nucl Med Mol Imaging* 2015;42:438–46. doi:10.1007/s00259-014-2955-8.
- [49] Knezevic D, Verhoeff NPL, Hafizi S, Strafella AP, Graff-Guerrero A, Rajji T, et al. Imaging microglial activation and amyloid burden in amnesic mild cognitive impairment. *J Cereb Blood Flow Metab* 2017;271678X17741395. doi:10.1177/0271678X17741395.
- [50] Fan Z, Dani M, Femminella GD, Wood M, Calsolaro V, Veronese M, et al. Parametric mapping using spectral analysis for 11C-PBR28 PET reveals neuroinflammation in mild cognitive impairment subjects. *Eur J Nucl Med Mol Imaging* 2018;45:1432–41. doi:10.1007/s00259-018-3984-5.

Figure legends

Figure 1. Flowchart illustrating the literature search strategy.

Figure 2. Overall standardised mean difference for each region of interest model in the comparison between HC and AD subjects (left) and HC and MCI subjects (right). Detailed model reports are presented in Tables 2 and 3.

Figure 3. Scatterplot demonstrating the association of AD MMSE score with standardised mean difference values in the parietal region. The size of study points is proportional to their precision. Lines presented are average predicted values with 95% confidence intervals (dashed lines).

Table 1. Characteristics of included studies.

Study	Ligand	Outcome	Subjects (n)			Age (mean & SD)			Female (%)			MMSE (mean & SD)		
			HC	MCI	AD	HC	MCI	AD	HC	MCI	AD	HC	MCI	AD
Groom et al., 1995 [12]	[11C]PK11195	Normalised binding	7	N/A	8	42- 78*	N/A	69- 80*	?	N/A	63	?	N/A	6-23*
Cagnin et al., 2001 [19]	[11C](R)- PK11195	Binding potential	15	N/A	8	57 (21)†	N/A	65.1 (6.1)	47	N/A	50	?	N/A	17 (6.4)
Kropholler et al., 2007 [21]	[11C](R)- PK11195	Binding potential	10	10	9	70 (6)	74 (6)	71 (6)	40	40	33	29 (1)	26 (1)	22 (3)
Edison et al., 2008 [41]	[11C](R)- PK11195	Binding potential	10	N/A	13	64.2 (5.5)	N/A	65.6 (4.6)	40	N/A	38	30	N/A	21.2 (3.9)
Tomasi et al., 2008 [22]	[11C](R)- PK11195	Binding potential	10	N/A	10	?	N/A	?	?	N/A	?	?	N/A	?
Yasuno et al., 2008 [42]	[11C]DAA1106	Binding potential	10	N/A	10	67.9 (5)	N/A	70.2 (7.4)	30	N/A	50	29.7 (0.67)	N/A	20.6 (2.67)

Okello et al., 2009 [8]	[11C](R)- PK11195	Binding potential	10	13	N/A‡	60.2 (9.3)	66.6 (9.6)	N/A‡	40	36	N/A‡	29.9 (0.3)	27.7 (1.5)	N/A‡
Wiley et al., 2009 [14]	[11C](R)- PK11195	Region of interest to subcortical white matter ratio (atrophy corrected)	5	6	6	72.0 (5.9)	71.8 (8.5)	76.5 (10.5)	40	33	33	29.4 (0.9)	28.7 (1.0)	19.3 (4.8)
Gulyás et al., 2011 [13]	[11C]Vinpocetine	Standardized uptake values	6	N/A	6	67.3 (7.6)	N/A	73.4 (6.2)	0	N/A	50	?	N/A	?
Yokokura et al., 2011 [43]	[11C](R)- PK11195	Binding potential	10	N/A	11	?	N/A	70.6 (6.4)	?	N/A	45	?	N/A	21.5 (3.5)
Yasuno et al., 2012 [44]	[11C]DAA1106	Binding potential	10	7	N/A§	67.9 (5)	67.1 (10.7)	N/A§	30	43	N/A§	29.7 (0.7)	28.6 (1.3)	N/A§
Kreisl et al., 2013 [45]	[11C]PBR28	Distribution volume corrected for free	13	10	19	62.9 (6.4)	72.6 (9.7)	63.1 (8.8)	31	40	42	29.8 (0.4)	27.5 (2)	20.3 (4.2)

		fraction of radioligand in plasma (partial volume corrected)												
Schuitemaker et al., 2013 [46]	[11C](R)- PK11195	Binding potential	21	10	19	68 (8)	72 (6)	69 (8)	38	30	42	29 (1)	26 (1)	23 (3)
Varrone et al., 2013 [15]	[18F]FEDAA1106	Binding potential	7	N/A	9	68 (3)	N/A	69 (4)	29	N/A	33	29 (1)	N/A	25 (3)
Fan et al., 2015 [47]	[11C](R)- PK11195	Binding potential	8	10	10	65.5 (5.5)	67.7 (7.7)	66.3 (6.1)	50	50	60	30	28.2 (1.8)	20.5 (4.2)
Golla et al., 2015 [16]	[18F]DPA-714	Binding potential	6	N/A	9	64.5 (5.5)	N/A	73.6 (8.4)	83	N/A	44	28.8 (0.8)	N/A	24.6 (2.8)
Lyoo et al., 2015 [38]	[11C]PBR28	Standardized uptake value ratio	21	11	25	55.1 (15.3)	72.2 (9.3)	63.0 (8.3)	29	36	56	?	?	?

Suridjan et al., 2015 [23]	[18F]FEPPA	Total distribution volume (partial volume error corrected)	21	N/A	18	61.3 (9.9)	N/A	68.3 (9.4)	57	N/A	48	29.4 (0.9)	N/A	17.5 (7)
Varrone et al., 2015 [48]	[18F]FEMPA	Total distribution volume	7	N/A	10	64 (7)	N/A	67 (7)	57	N/A	50	29.3 (1.0)	N/A	25.5 (2.5)
Femminella et al., 2016 [17]	[11C](R)- PK11195	Binding potential	8	N/A	8	65.9 (6.2)	N/A	66.2 (6.4)	25	N/A	38	29.4 (0.9)	N/A	19 (5.3)
Hamelin et al., 2016 [30]	[18F]DPA-714	Standardized uptake value ratio	20	34	24	68.2 (8.4)	67.8 (9.1)	68.3 (12.1)	75	58	69	29.5 (0.6)	24.1 (2.8)	15.8 (4.5)
Knezevic et al., 2017 [49]	[18F]FEPPA	Standardized uptake value ratios (partial volume error corrected)	14	11	N/A	67.1 (6.5)	71.9 (5.3)	N/A	64	55	N/A	29.3 (1.3)	27.3 (2.0)	N/A
Kreisl et al., 2017 [39]	[11C]PBR28	Standardized uptake value ratio	15	N/A	11	63.7 (4.7)	N/A	65.6 (7.3)	20	N/A	45	29.9 (0.4)	N/A	21.5 (4.7)

Parbo et al., 2017 [20]	[11C](R)- PK11195	Binding potential	10	26	N/A	68.3 (6.6)	73.3 (6.2)	N/A	60	35	N/A	29 (25- 30)¶	27 (23- 30)¶	N/A
Yokokura et al., 2017 [28]	[11C]DPA713	Binding potential	12	N/A	7	71.6 (2.6)	N/A (7.4)	69.3	58	N/A	86	28.3 (1.1)	N/A	19.4 (2.9)
Yokokura et al., 2017 [28]	[11C](R)- PK11195	Binding potential	10	N/A	10	72.2 (8.1)	N/A (6.7)	70.8	60	N/A	50	29.5 (1.0)	N/A	22.1 (3.5)
Fan et al., 2018 [50]	[11C]PBR28	Impulse response function	9	13	N/A	65.4 (7.5)	70.9 (8.1)	N/A	?	?	N/A	29.4 (1.0)	26.8 (2.9)	N/A
Passamonti et al., 2018 [24]	[11C]PK11195	Binding potential	13	7	9	68.0 (5.5)	70.3 (5.0)	67.4 (10.5)	62	71	22	28.7 (1.0)	26.6 (1.8)	24.6 (3.5)

* Range.

† Median and inter-quartile range.

‡ Removed from analysis because they contained the same subjects as in Edison et al., 2008.

§ Removed from analysis because they contained the same subjects as in Yasuno et al., 2008.

¶ Median and range.

Table 2. Random effects meta-analyses results, stratified by region of interest, between HC and AD subjects.

Region	Number of studies	Subjects			Overall effect		Heterogeneity	
		HC	AD	SMD [95% CI]	Z	P	I ²	P
Amygdala	5 [19,24,28,46]	71	53	1.17 [0.48 - 1.85]	3.34	0.001	65.5%	0.017
Cingulate (Anterior)	13 [15,17,19,22,24,28,30,41–43,45,47]	146	148	0.81 [0.42 - 1.19]	4.14	<0.001	57.3%	0.006
Cingulate (Posterior)	16 [14,15,17,19,22,24,28,30,41–43,45–48]	179	183	0.84 [0.51 - 1.17]	4.98	<0.001	53.4%	0.004
Caudate	6 [15,16,24,28,48]	55	54	0.39 [-0.54 - 1.32]	0.82	0.413	81.1%	0.001
Cerebellum	13 [13–16,19,22–24,28,38,42,48]	143	137	0.45 [0.06 - 0.83]	2.27	0.023	57.1%	0.006
Cortex	3 [12,17,41]	25	29	0.61 [-0.74 - 1.96]	0.88	0.376	81.3%	0.006
Frontal	9 [14–17,30,41,46–48]	92	108	0.57 [0.19 - 0.95]	2.96	0.003	37.1%	0.088
Middle frontal	5 [22,24,28,43]	55	47	1.60 [1.08 - 2.12]	6.04	<0.001	23.0%	0.236
Orbitofrontal cortex	2 [15,24]	20	18	0.76 [0.10 - 1.43]	2.24	0.025	0.0%	0.853
Prefrontal cortex	6 [13,19,23,39,42,45]	80	72	0.94 [0.60 - 1.28]	5.38	<0.001	0.0%	0.416
Superior frontal	4 [24,28,43]	45	37	1.31 [0.42 - 2.19]	2.90	0.004	68.6%	0.033
Grey matter	2 [15,16]	13	18	0.02 [-0.70 - 0.74]	0.05	0.961	0.0%	0.396
Insula	4 [15,16,19,24]	41	35	0.30 [-0.17 - 0.77]	1.26	0.209	0.0%	0.562

Midbrain	2 [15,24]	20	18	0.24 [-1.07 - 1.55]	0.36	0.716	73.9%	0.050
Occipital	17 [13,15–17,22–24,28,30,38,39,41,42,46–48]	205	208	0.82 [0.50 - 1.14]	5.06	<0.001	55.5%	0.003
Lingual gyrus	2 [22,24]	23	19	0.55 [-0.57 - 1.67]	0.96	0.339	67.9%	0.078
Pallidum	2 [19,24]	28	17	0.74 [0.09 - 1.39]	2.23	0.026	6.7%	0.301
Parietal	15 [13–17,22,23,28,30,41,42,46–48]	161	169	0.77 [0.46 - 1.09]	4.81	<0.001	44.1%	0.028
Inferior parietal	4 [19,24,38,39]	64	53	1.26 [0.75 - 1.76]	4.87	<0.001	32.5%	0.251
Superior parietal	3 [22,24,39]	38	30	1.05 [0.39 - 1.70]	3.13	0.002	37.0%	0.202
Precuneus	7 [24,28,30,38,39,43]	101	97	1.34 [0.72 - 1.97]	4.24	<0.001	72.8%	0.002
Pons	4 [15,19,24,48]	42	36	0.49 [0.02 - 0.95]	2.06	0.039	0.0%	0.470
Putamen	7 [15,16,19,24,28,48]	70	62	0.63 [-0.06 - 1.32]	1.79	0.074	70.7%	0.005
Sensorimotor cortex	3 [12,14,45]	25	33	0.16 [-0.60 - 0.91]	0.41	0.684	46.0%	0.162
Striatum	5 [13,17,41,42,45]	47	56	0.72 [0.10 - 1.35]	2.26	0.024	54.9%	0.068
Temporal	7 [15–17,23,30,41,47]	80	91	0.92 [0.49 - 1.34]	4.18	<0.001	40.0%	0.107
Entorhinal	3 [38,39,46]	57	55	1.07 [0.14 - 2.00]	2.25	0.024	80.3%	0.018
Hippocampus	14 [15–17,19,23,24,28,30,38,39,43,46,47]	187	178	0.74 [0.35 - 1.13]	3.72	<0.001	66.6%	0.001

Inferior and middle temporal	4 [19,24,38,39]	64	53	1.76 [0.97 - 2.56]	4.36	<0.001	67.2%	0.015
Lateral temporal	6 [13,28,42,46,48]	66	62	0.95 [0.08 - 1.82]	2.13	0.033	79.8%	0.001
Medial temporal	6 [13,14,17,24,42,48]	49	49	0.71 [0.29 - 1.12]	3.33	0.001	0.0%	0.401
Parahippocampal	6 [19,24,28,38,43]	81	70	1.33 [0.67 - 1.99]	3.93	<0.001	68.2%	0.012
Posterior temporal	2 [22,24]	23	19	1.41 [0.73 - 2.09]	4.04	<0.001	0.0%	0.464
Superior temporal	5 [19,24,39,45,46]	77	66	0.83 [0.36 - 1.30]	3.46	0.001	42.6%	0.137
Thalamus	17 [12,13,15-17,19,21-24,28,41,42,45,46,48]	186	182	0.43 [0.16 - 0.70]	3.07	0.002	37.7%	0.040
White matter	5 [12,15,16,45,48]	40	55	0.07 [-0.46 - 0.61]	0.27	0.791	37.9%	0.150

Table 3. Random effects meta-analyses results, stratified by region of interest, between HC and MCI subjects

Region	Number of studies	Subjects		SMD [95% CI]	Overall effect		Heterogeneity	
		HC	MCI		Z	P	I ²	P
Amygdala	3 [24,46,50]	43	30	0.90 [-0.41 - 2.21]	1.35	0.176	83.6%	0.001
Cingulate (Anterior)	6 [8,24,30,44,45,47]	74	81	0.60 [0.13 - 1.08]	2.48	0.013	46.9%	0.095
Cingulate (Posterior)	10 [8,14,20,24,30,44–47,50]	119	136	0.70 [0.42 - 0.98]	4.86	<0.001	10.6%	0.412
Cerebellum	5 [14,24,38,44,50]	58	44	0.55 [-0.00 - 1.11]	1.95	0.051	42.2%	0.149
Frontal	7 [8,14,20,30,46,47,50]	83	112	0.66 [0.36 - 0.97]	4.31	<0.001	0.0%	0.653
Prefrontal cortex	3 [44,45,49]	37	28	0.40 [-0.17 - 0.97]	1.38	0.168	21.3%	0.270
Occipital	8 [24,30,38,44,46,47,49,50]	116	103	0.58 [0.29 - 0.86]	3.94	<0.001	3.2%	0.471
Parietal	8 [8,14,20,30,44,46,47,50]	93	119	0.75 [0.42 - 1.07]	4.53	<0.001	15.2%	0.285
Inferior parietal	3 [24,38,49]	48	29	0.37 [-0.09 - 0.84]	1.56	0.118	0.0%	0.696
Precuneus	4 [20,24,30,38]	64	78	0.90 [0.39 - 1.41]	3.47	<0.001	45.1%	0.142
Sensorimotor cortex	2 [14,45]	18	16	0.00 [-0.68 - 0.68]	-0.01	0.991	0.0%	0.459
Striatum	3 [44,45,50]	32	30	0.48 [-0.37 - 1.32]	1.11	0.269	61.2%	0.082
Temporal	5 [8,30,47,49,50]	61	81	0.87 [0.52 - 1.23]	4.87	<0.001	0.0%	0.443

Entorhinal	2 [38,46]	42	21	0.24 [-0.28 - 0.77]	0.91	0.365	0.0%	0.548
Hippocampus	7 [24,30,38,46,47,49,50]	106	96	0.46 [0.17 - 0.76]	3.12	0.002	0.0%	0.487
Inferior and middle temporal	2 [24,38]	34	18	0.30 [-0.28 - 0.88]	1.02	0.309	0.0%	0.384
Lateral temporal	3 [20,44,46]	41	43	0.74 [0.04 - 1.45]	2.06	0.040	52.3%	0.123
Medial temporal	5 [14,20,24,44,50]	47	59	0.80 [0.38 - 1.22]	3.75	<0.001	0.0%	0.545
Parahippocampal	2 [24,38]	34	18	0.45 [-0.17 - 1.08]	1.41	0.157	12.1%	0.286
Superior temporal	3 [24,45,46]	47	27	0.18 [-0.31 - 0.66]	0.71	0.475	0.0%	0.318
Thalamus	6 [21,24,44-46,50]	76	57	0.50 [0.14 - 0.86]	2.74	0.006	0.0%	0.550
Whole brain	2 [8,50]	19	26	0.77 [0.15 - 1.38]	2.44	0.015	0.0%	0.540